Journal of Power Sources 265 (2014) 57–61

Contents lists available at ScienceDirect

Journal of Power Sources

journal homepage: www.elsevier.com/locate/jpowsour

Short communication

Acrylonitrile-contamination induced enhancement of formic acid electro-oxidation at platinum nanoparticles modified glassy carbon electrodes

Gumaa A. El-Nagar [a], Ahmad M. Mohammad [a,b], Mohamed S. El-Deab [a,b,c,*], Takeo Ohsaka [c], Bahgat E. El-Anadouli [a]

[a] Chemistry Department, Faculty of Science, Cairo University, Cairo 12613, Egypt
[b] Department of Chemical Engineering, Faculty of Engineering, The British University in Egypt, Cairo 11837, Egypt
[c] Department of Electronic Chemistry, Interdisciplinary Graduate School of Science and Engineering, Tokyo Institute of Technology, Midori-ku, 4259 Nagatsuta, Yokohama 226-8502, Japan

HIGHLIGHTS

- FAO is unexpectedly enhanced at nano-Pt/GC electrodes poisoned with AcN.
- The extent of enhancement depends on the surface coverage (θ) of AcN.
- AcN favors the direct FAO at the expense of the indirect oxidation (CO pathway).
- Adsorption of AcN impurities alters the electronic properties of the underlying Pt surface.

ARTICLE INFO

Article history:
Received 24 January 2014
Received in revised form
6 April 2014
Accepted 23 April 2014
Available online 2 May 2014

Keywords:
Formic acid fuel cell
Impurities
Nanoparticles
Carbon monoxide
XPS

ABSTRACT

Minute amount (~1 ppm) of acrylonitrile (AcN), a possible contaminant, shows an unexpected enhancement for the direct electro-oxidation of formic acid (FAO) at Pt nanoparticles modified GC (nano-Pt/GC) electrodes. This is reflected by a remarkable increase of the current intensity of the direct oxidation peak (I_p^d, at ca. 0.3 V) in the presence of AcN, concurrently with a significant decrease of the second (indirect) oxidation current (I_p^{ind}, at ca. 0.7 V), compared to that observed in the absence of AcN (i.e., at the unpoisoned Pt electrode). The extent of enhancement depends on the surface coverage (θ) of AcN at the surface of Pt nanoparticles. AcN is thought to favor the direct FAO by disturbing the contiguity of the Pt sites, which is necessary for CO adsorption. Furthermore, XPS measurements revealed a change in the electronic structure of Pt in presence of AcN, which has a favorable positive impact on the charge transfer during the direct FAO.

1. Introduction

Fuel cells have been emerged as a clean, efficient, reliable and durable electrical energy supply systems replacing the fossil fuels. In this regard, the direct formic acid fuel cells (DFAFCs) have shown superiority over the traditional hydrogen (HFCs) and direct methanol (DMFCs) fuel cells in providing electricity for portable electronic devices. This advantage is acquired from the easiness and safety concerns associated with storing and transporting formic acid (FA). Moreover, the slow crossover of FA through the Nafion-based membranes and the reasonable oxidation kinetics of FA have also enriched the desire to DFAFCs [1–3]. The electro-oxidation of FA (FAO) is the essential anodic reaction in DFAFCs. So far, Pd-based and Pt-based electrodes are among the best catalysts for this reaction, nevertheless, Pd suffers from an inherent instability [2,4–8] and Pt electrodes suffer from the CO poisoning.

Generally, FAO on Pt-based electrodes follows a dual (direct and indirect) pathway mechanism. The direct (desirable) pathway involves the dehydrogenation of FA to CO_2 at relatively low anodic potential (with a peak current I_p^d). On the other hand, the indirect (dehydration) pathway involves a non-faradaic dissociation of FA to CO (undesirable) which is adsorbed at the Pt surface and subsequently oxidized at higher potential (with a peak current I_p^{ind}). The

* Corresponding author. Chemistry Department, Faculty of Science, Cairo University, Cairo 12613, Egypt.
E-mail address: msaada68@yahoo.com (M.S. El-Deab).

http://dx.doi.org/10.1016/j.jpowsour.2014.04.116
0378-7753/

adsorption of CO on Pt surface causes a surface poisoning and thus impedes the direct oxidation pathway of FA to CO_2 [9–16]. The decoration of the surface of the Pt electrode with other metal and/or metal oxides is shown to overcome/reduce the CO poisoning and improve the electrode catalytic activity, mainly due to a favorable geometric and/or electronic modification which disfavors the CO adsorption. For instance, interruption of the Pt site contiguity by gold nanoparticles (AuNPs) could eventually hinder the CO adsorption leading to an outstanding electrocatalytic activity towards the direct FAO without passing by the CO intermediate [17–19]. Additionally, metal oxides could easily provide/exchange oxygen species which facilitate the oxidative removal of CO at reasonable potentials [2,6–8].

In order to commercialize the DFAFCs, the high price and the deterioration of the catalytic activity of the costly Pt catalyst should be overcome. In fact, the major influence for the efficiency loss in DFAFCs comes from the deterioration of the catalytic activity of the Pt catalyst by inevitable organic and/or inorganic contaminants, e.g., nitrogen- and/or sulfur-containing compounds (entering the cell with air), halides (where most of the high-surface area fuel cell catalysts are often synthesized from halide-containing educts), and hydrocarbons (if any defect appeared in piping, blowers, pumps and heat exchangers) [20–22]. Basically, the existence of these organic compounds at the Pt surface is able to alter the binding energies of Pt with key intermediates, which ultimately influence the reaction kinetics [23]. St-Pierre et al. [24] reported a significant loss in PEMFCs performance in the presence of some airborne hydrocarbon contaminants (e.g., acetonitrile and toluene), which is restored back after exposure to clean air. Moreover, acrylonitrile (AcN) is shown as a possible hydrocarbon contaminant from the materials making up the balance of plant (BOP) of PEMFCs such as accessories, piping, blowers, pumps and heat exchanger [21]. A severe poisoning for the kinetics of the oxygen reduction reaction was observed in the presence of a minute amount (~ppm) of AcN at commercially available Pt/C catalysts in O_2-saturated 0.1 M $HClO_4$ solution [20]. In this context, the investigation of the impact of AcN on the catalytic performance of the anodic part of PEMFCs has a prime importance.

Herein, unpredictable surprising enhancement for the direct FAO at Pt nanoparticles modified GC (nano-Pt/GC) electrodes is observed in the presence of a minute amount (in ppm) of AcN. The catalytic enhancement is shown to depend on the AcN concentration. The results are explained in view of the possible reaction pathways of FAO with the help of XPS measurements.

2. Experimental

Glassy carbon (GC, $d = 3.0$ mm) and Pt ($d = 1.6$ mm) electrodes (from ALS-Japan) were used as working electrodes after polishing with aqueous slurries of successively finer alumina powder on a microcloth. The Pt electrodes were further electrochemically cleaned by scanning the potential between the onset potentials of the HER and OER in 0.5 M H_2SO_4 for several cycles until the characteristic cyclic voltammogram (CV) of a clean Pt surface was obtained. A spiral Pt wire and Ag/AgCl/KCl (sat) were used as the counter and reference electrodes, respectively.

The electrodeposition of PtNPs on the bare GC (nano-Pt/GC) electrode was done in 0.1 M H_2SO_4 containing 1.0 mM $H_2[PtCl_6]$ solution at a constant potential of 1 V for 300 s. This typically ends up with ca. 55 μg Pt loading (7.85×10^{-4} g cm^{-2}), as estimated from the amount of charge passed during the potentiostatic electrodeposition of Pt.

The electrochemical measurements were performed at room temperature (25 ± 1 °C) in a conventional two-compartment three-electrode glass cell using an EG&G potentiostat (model 273A) operated with Echem 270 software. The electrocatalytic activity of the nano-Pt/GC electrode towards FAO was examined by measuring cyclic voltammograms (CVs) in 0.5 M H_2SO_4 containing 0.3 M FA in presence/absence of AcN (in ppm range). The real surface areas were evaluated in two ways; using the hydrogen adsorption/desorption peaks and using the CO stripping peak. Current densities are calculated on the basis of the geometric surface area of the working electrode (geometric area = 0.07 cm^2). A field emission scanning electron microscope (FE-SEM, QUANTA FEG 250) coupled with an energy dispersive X-ray spectrometer (EDX) unit was employed to evaluate the electrode morphology and composition. X-ray photoelectron spectroscopy (XPS, operating with Al Kα radiation) was employed in the determination of the electronic structure of the Pt catalyst. The binding energies derived from XPS measurements have been calibrated to the C1s spectrum (at 284.5 eV) of the carbon support.

3. Results and discussions

Fig. 1A shows an SEM micrograph for the nano-Pt/GC electrode, in which Pt nanoparticles with an average particle size of 80 nm are homogenously covering the entire GC surface. A typical characteristic CV for a Pt substrate measured in 0.5 M H_2SO_4 is observed with a broad oxidation peak for the Pt-oxide formation (commences at ca. 0.65 V and extends up to 1.4 V) coupled with a single reduction peak centered at ca. 0.45 V (Fig. 1B, curve a). The hydrogen adsorption/desorption ($H_{ads/des}$) couple appeared in the potential

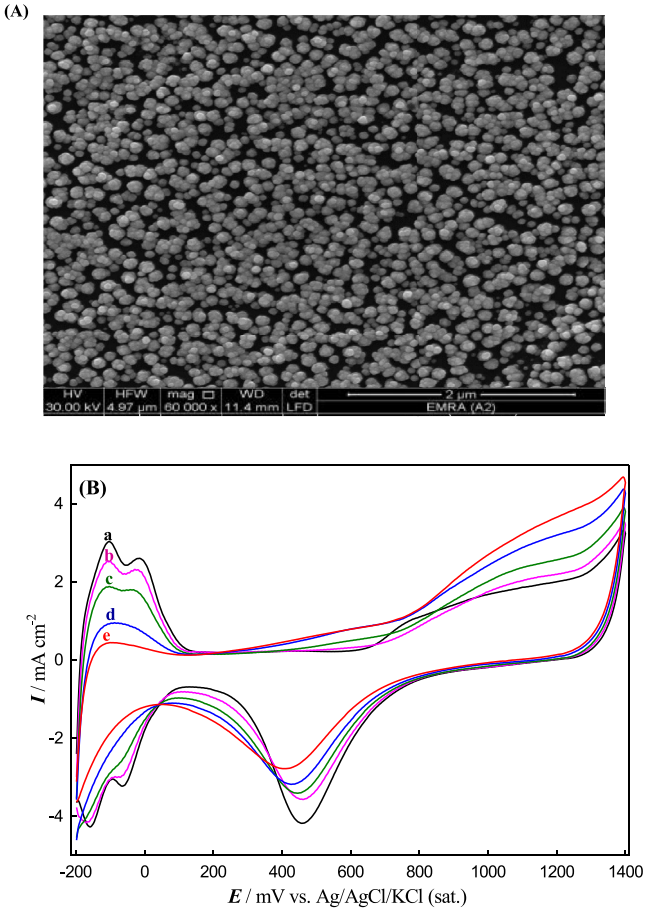

Fig. 1. (A) SEM micrograph for nano-Pt/GC. (B) CVs of the nano-Pt/GC electrode in 0.5 M H_2SO_4 solution containing (a) 0, (b) 1, (c) 10, (d) 30, and (e) 50 ppm AcN. Potential scan rate: 100 mV s^{-1}.

Table 1
Effect of AcN concentration on the peak current of direct (I_p^d) and indirect (I_p^{ind}) oxidation of FA, oxidation capacity (OC) and onset potential (E_{onset}) of the direct FA oxidation at nano-Pt/GC electrode in 0.3 M FA + 0.5 M H_2SO_4.

[AcN]/ppm	I_p^d/μA	I_p^{ind}/μA	I_p^d/I_p^{ind}	OC	E_{onset}/mV	θ_{AcN}
0	137	188	0.7	9.6×10^2	−55	0.0
1	282	69	4.0	2.9×10^3	−222	15
10	323	28	12	6.8×10^3	−256	20
20	442	2	221	2.3×10^4	−259	28
30	497	0.1	4970	5.2×10^4	−260	41
50	461	–	–	9.8×10^4	−278	87
70	407	–	–	4.3×10^5	−232	93
90	342	–	–	2.1×10^6	−218	95
100	292	–	–	2.9×10^7	−201	98

region from −0.2 to 0.2 V for the nano-Pt/GC electrode in the absence of AcN. The same features were observed for the nano-Pt/GC electrode in the presence of AcN (albeit with lower currents) with the appearance of a broad oxidation peak between 1.2 and 1.4 V (overlapped with the Pt-oxide formation peak) corresponding to the oxidation of adsorbed AcN (Fig. 1B, curves b–e) [20]. The noticeable decrease in the intensity of the Pt-oxide reduction peak and the intensity of the $H_{ads/des}$ peaks points to a decrease in the Pt surface area due to the adsorption of AcN. In the absence of AcN, the real surface area of Pt in the nano-Pt/GC electrode is estimated (0.14 cm^2) from the H_{des} peak (using a reported value of 210 μC cm^{-2}) [25].

The surface coverage (θ) of AcN on nano-Pt/GC catalyst has been estimated from the decrease of the charge of the H_{des} peaks. A systematic increase in θ is observed with increasing AcN concentration (see Table 1).

The electrocatalytic activity of the nano-Pt/GC electrode in the presence of various concentrations of AcN was performed in 0.5 M H_2SO_4 containing 0.3 M FA (see Fig. 2A). This figure shows that, in the absence of AcN, nano-Pt/GC (curve a) two oxidation peaks of FA in the forward scan at ca. 0.3 and 0.68 V, respectively. The first peak corresponds to the direct oxidation of FA to CO_2 (with a peak current I_p^d), while the second peak at ∼0.68 V is attributed to the oxidation of the poisonous adsorbed species (CO_{ads}) to CO_2 (with a peak current I_p^{ind}).

Surprisingly, in the presence of 1 ppm AcN (as impurity), the FAO at nano-Pt/GC electrode (curve b) exhibited a noticeable increase in I_p^d with a concurrent depression of I_p^{ind}. Additionally, a large negative shift in the onset potential of the direct FAO by ca. 0.2 V towards the negative direction of potential is obtained (compare curves a and b). Therefore, the addition of AcN causes a catalytic enhancement for the direct FAO in terms of increased oxidation current and favorable shift in potential. To that extent, the indirect peak (corresponding to the oxidation of CO_{ads}) completely ceased in the presence of 30 ppm AcN (θ = 41%). The ratio of the charge involved in the direct FAO (Q_d) to the total charge of both the direct and indirect FAO (Q_t) approached unity similar to the FAO at Pd-based anodes [4]. This unpredicted enhancement is opposite to that observed for the case of the ORR [20], in which minute amounts of AcN could remarkably suppress the catalytic activity of the ORR at Pt/C catalyst [20].

It should be mentioned here that I_p^d increases initially with AcN concentration (≤30 ppm) and then decreases (>30 ppm), see Table 1. Note that the active surface for the FAO is that of Pt and the number of active sites of Pt available for the FAO determines the rate of the direct reaction (i.e., the value of I_p^d). A 30 ppm AcN (θ = 40%) seems optimum and for $\theta > 40\%$, the number of Pt sites available for FAO decreases and thus I_p^d as well.

Fig. 2B shows the ratio of Q_d/Q_t as a function of θ. As clearly seen, the ratio Q_d/Q_t increases with θ reaching its maximum value of unity at θ ca. 40%. If the number of free active sites of Pt decreases (due to AcN adsorption) one would expect a decrease in Q_d, which is opposite to the current observation. To understand this, AcN adsorption is believed to take place at the expense of CO adsorption, i.e., a competition between CO and AcN adsorption favors the adsorption of the later at the expense of the former. Note that, the

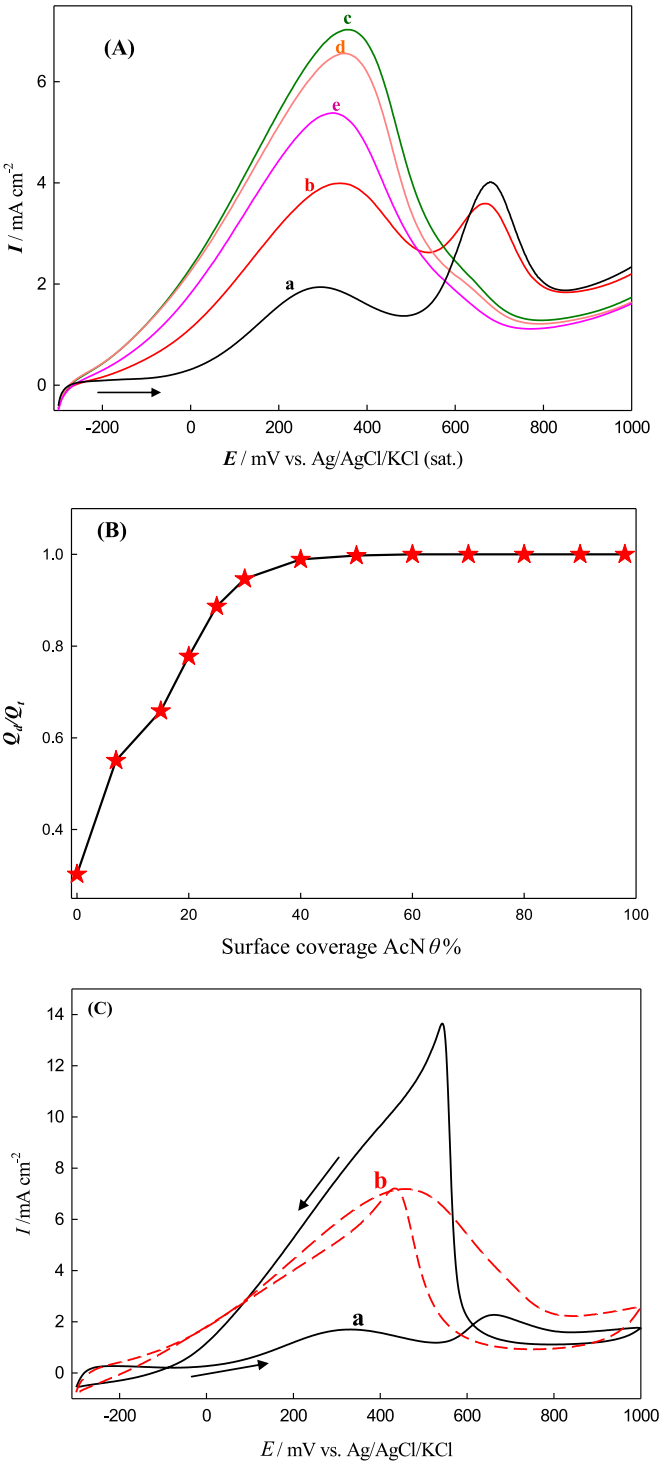

Fig. 2. (A) LSV for FAO at nano-Pt/GC electrode in 0.3 M FA + 0.5 M H_2SO_4 solution containing (a) 0, (b) 5, (c) 30, (d) 50 and (e) 70 ppm AcN. Potential scan rate: 100 mV s^{-1}. The arrow indicates the direction of the potential scan. (B) Variation of Q_d/Q_t with θ. (C) CVs for FAO at nano-Pt/GC electrode in 0.3 M FA + 0.5 M H_2SO_4 solution in the absence (a) and the presence (b) of 30 ppm AcN. Potential scan rate: 100 mV s^{-1}.

I_p^d/I_p^{ind} ratio increases from ca. 0.2 at nano-Pt/GC electrode in absence of AcN to ca. 220 in presence of 20 ppm AcN (θ = 28%). Table 1 lists the values of I_p^d/I_p^{ind} ratio obtained in the presence of various concentrations of AcN. The increase of I_p^d/I_p^{ind} (and Q_d/Q_t) with θ indicates a favorable improvement in the catalytic activity of the nano-Pt/GC electrode toward the direct FA oxidation by AcN, which might originate from retarding the CO adsorption and thus favoring the direct oxidation pathway. Fig. 2A shows only the positive-going potential scan (LSV), and Fig. 2C shows a complete CV for the FAO at nano-Pt/GC electrode in the absence (a) and the presence (b) of 30 ppm AcN.

An important catalytic index, "oxidation capacity (OC)", is developed which combines the charge consumed in the direct oxidation peak (Q_d) with the number of Pt active sites available for FAO.

$$OC = \frac{Q_d}{\text{number of Pt active sites}} \quad (1)$$

where the number of Pt active sites was estimated with the assumption that 1 cm^2 of Pt surface contains about 1.5×10^{15} atoms [26–28].The increase in OC means that the electrode has a significant CO tolerance and the direct FAO proceeds preferentially via the direct pathway (larger values of Q_d). Fig. 3A shows that the OC of FAO increases with θ. Note that the increase of AcN concentration

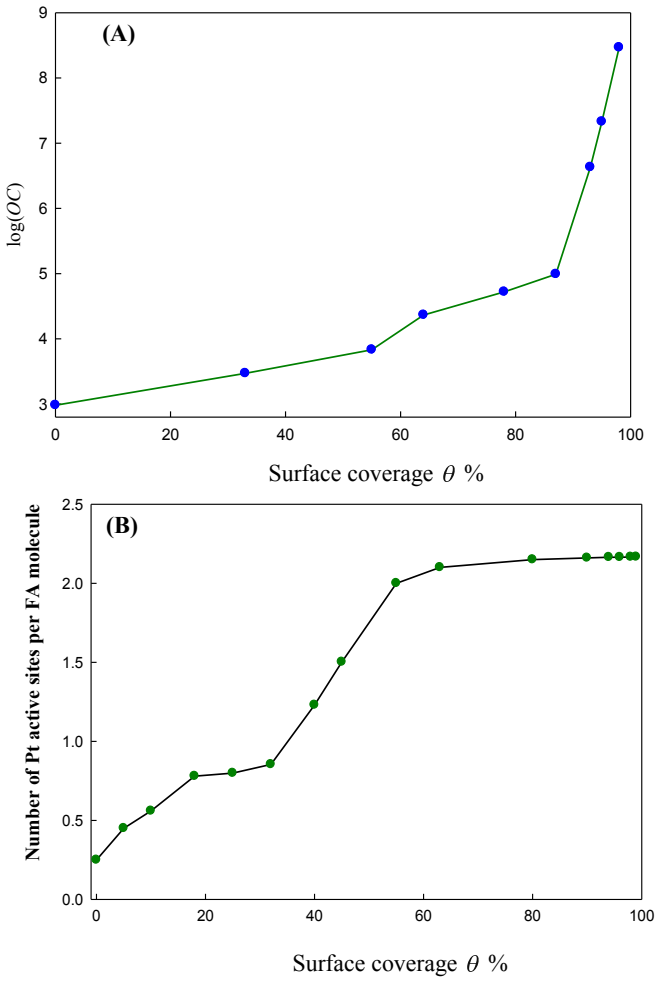

Fig. 3. (A) Variation of oxidation capacity (OC) of nano-Pt/GC electrode towards FAO with θ. (B) Variation of number of Pt active sites per FA molecule with θ.

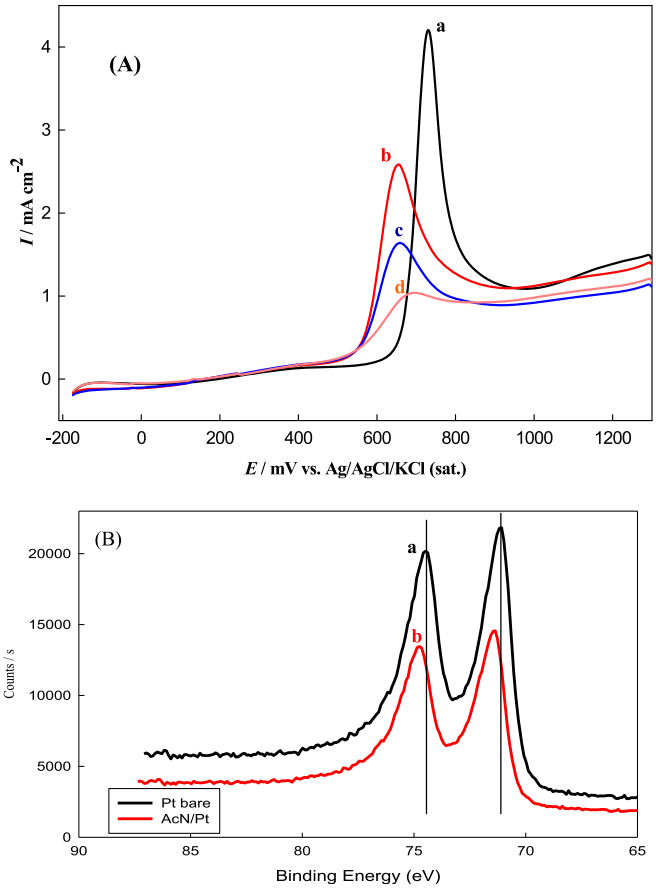

Fig. 4. (A) Oxidative stripping of CO at nano-Pt/GC in 0.5 M H_2SO_4 in the presence of (a) 0, (b) 5, (c) 20 and (d) 35 ppm AcN. Potential scan rate: 50 mV s^{-1}. (B) XPS spectra of Pt 4f in (a) the absence and (b) the presence of 100 ppm AcN.

(i.e., increase of θ) increases Q_d (see Fig. 2B). A plausible explanation might be that the adsorption of AcN prevents the deactivation of Pt sites by impeding the CO adsorption. It has been presumed that the adsorption of one CO molecule atop the Pt surface requires the existence of three adjacent Pt sites [17–19], thus the adsorption of AcN interrupts this contiguity and hence preventing/weakened the CO adsorption and consequently more Pt sites are being available for the direct FAO. At high θ values, the number of Pt active surface sites decreases substantially with a simultaneous decrease in Q_d to low insignificant values.

The number of molecules of FA was estimated from the amount of charge consumed in the direct FAO by considering the generation of 2-electrons per the oxidation of one FA molecule (see Equation (2)).

$$HCOOH \rightarrow CO_2 + 2H^+ + 2e^- \quad (2)$$

Inspection of Fig. 3B reveals two adsorption modes for FA at low and high θ of AcN at Pt surface. At low θ ($20 \leq \theta \leq 40\%$), a ratio close to 1:1 is obtained for Pt sites: FA molecules. The reason for this may originate from the availability of a plenty of active Pt sites for FAO. On the other hand, at high θ ($\geq$60%), a ratio close to 2:1 is obtained due to the high coverage of Pt surface with AcN causing a hindrance for FA adsorption. In this case, each FA molecule is apparently bound to two adjacent Pt sites. The change of the adsorption modes of reactants upon the modification of Pt surface has been previously proposed for the ORR at nano-MnOx/Pt electrode, where two adsorption modes were observed for oxygen molecule in presence and absence of nano-MnOx [29].

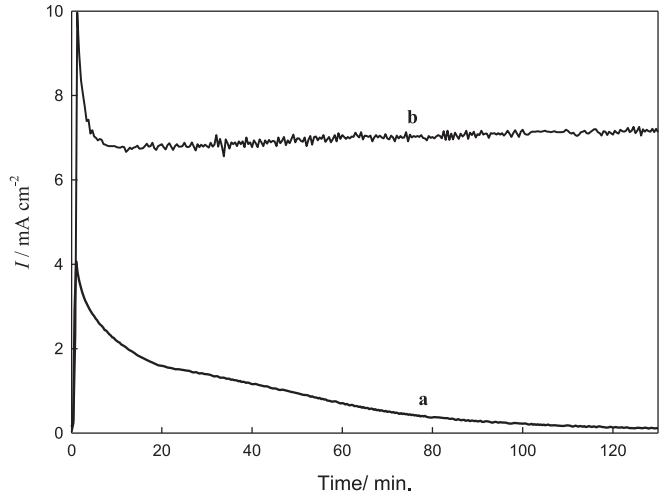

Fig. 5. Current transients (i–t curves) recorded at 0.3 V vs. Ag/AgCl for FAO in 0.3 M FA + 0.5 M H_2SO_4 at nano-Pt/GC electrode in (a) the absence and (b) the presence of 30 ppm AcN.

In order to verify the catalytic enhancement of the direct FA oxidation in the presence of AcN, CO was adsorbed at the nano-Pt/GC surface (at open circuit potential) in absence and presence of AcN. The oxidative stripping of CO is shown in Fig. 4A. This figure indicates a significant lowering in the intensity of the oxidation peak of CO in the presence of AcN with a slight shift in the oxidation potential of CO from ca. 0.75 V (in the absence of AcN, curve a) to ca. 0.6 V (in the presence of 5 ppm AcN, curve b). A systematic decrease of the CO oxidation peak current is observed with AcN concentration. This finding provides an evidence for the assumption that AcN prevents/impedes the adsorption of CO but not significantly enhancing its oxidative removal. Thus, one can safely argue that AcN enhanced the direct FAO (Equation (2) above) rather than enhancing the oxidative removal of CO. The observed negative shift in the onset potential of CO oxidation presumably originates from a modification in the electronic structure of Pt surface, which weakens the Pt–CO bonding [17]. XPS measurements confirmed this change in the electronic properties of Pt surface, where a positive shift in the binding energy of Pt 4f (+0.15 eV) was observed in the presence of AcN adsorption (Fig. 4B). This suggests a partial charge transfer from the Pt atoms to AcN, which modifies the electronic structure of Pt surface in such a way that the Pt–CO bonding weakens [30].

The stability of the nano-Pt/GC electrode towards FAO has been probed by measuring the i–t curves in the absence and the presence of AcN. The data are shown in Fig. 5. This figure depicts that in the absence of AcN (curve a), the current decays rapidly due to the accumulation of the poisoning CO_{ads} on the Pt surface. On the contrary, in the presence of 30 ppm AcN (curve b) the Pt catalyst showed a remarkably high oxidation current which is effectively unchanged over a prolonged period of 2 h of continuous electrolysis at 0.3 V. This indicates the sustainable tolerance of the Pt catalyst against CO poisoning in the presence of AcN.

4. Summary

This study revealed, for the first time, that the adsorption of minute amounts of AcN on nano-Pt/GC electrode enhances the direct FAO and suppresses the CO pathway of FAO at Pt-based catalyst. That is AcN is believed to adsorb onto the Pt surface and interrupt the geometrical contiguity of the Pt sites favorable for CO adsorption. The modification of the electronic properties of the Pt surface by adsorption of AcN (verified by XPS) weakened/impede the Pt–CO bonding; thus accelerate the direct FAO.

References

[1] S.M. Baik, J. Kim, J. Han, Y. Kwon, Int. J. Hydrogen Energy 45 (2011) 12583 and references therein.
[2] G.A. El-Nagar, A.M. Mohammad, M.S. El-Deab, B.E. El-Anadouli, J. Electrochem. Soc. 159 (2012) F249.
[3] S. Zhanga, Y. Shao, G. Yin, Y. Lin, J. Power Sources 195 (2010) 1103.
[4] K. Persson, A. Ersson, K. Jansson, N. Iverlund, S. Jaras, J. Catal. 231 (2005) 139.
[5] W.S. Jung, J. Han, S.P. Yoon, S.W. Nam, T.-H. Lim, S.-A. Hong, J. Power Sources 196 (2011) 4573.
[6] G.A. El-Nagar, A.M. Mohammad, M.S. El-Deab, B.E. El-Anadouli, Electrochim. Acta 94 (2013) 62.
[7] M.S. El-Deab, L.A. Kibler, D.M. Kolb, Electrocatalysis 2 (2011) 220.
[8] K. Ramesh, L. Chen, F. Chen, Y. Liu, Z. Wang, Y.-F. Han, Catal. Today 131 (2008) 477.
[9] M.S. El-Deab, L.A. Kibler, D.M. Kolb, Electrochem. Commun. 11 (2009) 776.
[10] G. Samjeské, A. Miki, S. Ye, M. Osawa, J. Phys. Chem. B 110 (2006) 16559.
[11] J.D. Lović, A.V. Tripković, S.L. Gojković, K.D. Popović, D.V. Tripković, P. Olszewski, A. Kowal, J. Electroanal. Chem. 581 (2005) 294.
[12] M. Osawa, K. Komatsu, G. Samjesk, T. Uchida, T. Ikeshoji, A. Cuesta, C. Gutirrez, Angew. Chem. Int. Ed. 50 (2011) 1159.
[13] G. Samjesk, M. Osawa, Angew. Chem. Int. Ed. 44 (2005) 5694.
[14] Y.X. Chen, M. Heinen, Z. Jusys, R.J. Behm, Angew. Chem. Int. Ed. 45 (2006) 981.
[15] W. Gao, J.E. Mueller, Q. Jiang, T. Jacob, Angew. Chem. Int. Ed. 51 (2012) 9448.
[16] K. Kunimatsu, H. Kita, J. Electroanal. Chem. 218 (1987) 155.
[17] M.D. Obradović, J.R. Rogan, B.M. Babic, A.V. Tripković, A.R. Gautam, V.R. Radmilovic, S.L. Gojković, J. Power Sources 197 (2012) 72.
[18] A. Cuesta, M. Escudero, B. Lanova, H. Baltruschat, Langmuir 25 (2009) 6500.
[19] I.M. Al-Akraa, A.M. Mohammad, M.S. El-Deab, B.E. El Anadouli, Int. J. Electrochem. Sci. 7 (2012) 3939.
[20] (a) M.S. El-Deab, F. Kitamura, T. Ohsaka, J. Power Sources 229 (2013) 65; (b) M.S. El-Deab, F. Kitamura, T. Ohsaka, J. Electrochem. Soc. 160 (2013) F651.
[21] K. Kobayashi, Y. Oono, M. Hori, ECS Meet. Abstr. MA2012-02 (2012) 1291.
[22] B.D. Gould, O.A. Baturina, K.E. Swider-Lyons, J. Power Sources 188 (2009) 89.
[23] W. Zhu, B.A. Rosen, A. Salehi-Khojin, R.I. Masel, Electrochim. Acta 96 (2013) 18.
[24] J. St-Pierre, M.S. Angelo, Y. Zhai, ECS Trans. 41 (2011) 279.
[25] S. Trasatti, O.A. Petrii, Pure Appl. Chem. 93 (1991) 711.
[26] H.A. Laitinen, C.G. Enke, J. Electrochem. Soc. 107 (9) (1960) 773.
[27] K.J. Mayrhofer, D. Strmcnik, B. Blizanac, V. Stamenkovic, M. Arenz, N.M. Markovic, Electrochim. Acta 53 (2008) 3181.
[28] G.A. Somorjai, Introduction to Surface Chemistry and Catalysis, second ed., Wiley, New York, 2010.
[29] M.S. El-Deab, T. Ohsaka, Angew. Chem. Int. Ed. 45 (2006) 5963.
[30] V.M. Geskin, R. Lazzaroni, M. Mertens, R. Jérôme, J.L. Brédas, J. Chem. Phys. 105 (1996) 3278.